

Technical Notes

TECHNICAL NOTES are short manuscripts describing new developments or important results of a preliminary nature. These Notes cannot exceed 6 manuscript pages and 3 figures; a page of text may be substituted for a figure and vice versa. After informal review by the editors, they may be published within a few months of the date of receipt. Style requirements are the same as for regular contributions (see inside back cover).

Bubble Dynamics on a Heated Surface

Nasser Rashidnia*

NASA Lewis Research Center, Cleveland, Ohio 44135

Introduction

MANY studies of thermocapillary-induced motions near bubbles attached to a heated wall in conjunction with low-gravity space experiments have been performed in recent years. The relevance of Marangoni convection in materials processing and fluid management in space has been reviewed by Ostrach.¹ This interaction of gas and vapor bubbles with surrounding liquids is of great interest because the pronounced effects of capillary forces in a reduced gravity environment play a significant role in materials processing, fluid management, and boiling processes in space. On Earth, this interaction leads to a fluid motion brought about by two coexisting and sometimes competing mechanisms: 1) natural convection induced by the volumetric buoyancy force and 2) Marangoni convection driven by the interfacial stresses along the bubble surface. On Earth, volumetric forces dominate in systems with large volume to surface area ratios, but in the microgravity conditions of orbiting spacecraft the surface forces become more important. Understanding the intricacies of Marangoni convection is not only essential for space processing, but may also be extremely beneficial in controlling ground-based experiments and interpreting their results. Numerous reports have investigated the importance of thermocapillary flows.^{2–6} Young et al.² were the first to analyze thermocapillary migration of bubbles and droplets.

The need for major research in the area of the interaction of bubbles with solid interfaces in low-gravity environments was demonstrated by Papazian and Wilcox.⁷ Recently, interest in the thermocapillary flow near bubbles attached to a heated or cooled solid surface has increased, particularly in microgravity applications.^{8–11} Neither theoretical nor numerical^{12,13} results agree with recent experimental observations. Raake et al.⁸ and Chun et al.⁹ experimentally visualized thermal oscillations at Marangoni numbers above 6830.

To enhance our understanding and to resolve some inconsistencies in the previously mentioned reports, we have conducted a preliminary investigation of temperature and flow-fields in the vicinity of a bubble attached to a heated surface. While the results of such studies may not apply specifically to fluid handling, boiling, or materials processing, the understand-

ing generated will directly impact future investigations into these fields.

Parametric Definitions and Physical Considerations

Analysis and nondimensionalization of the continuity, momentum, energy equations, and experimental observations^{10,11} show that the important parameter group for this problem is the Marangoni number $Ma = RePr = (\rho l u_m / \mu)(\nu / \alpha)$, where Re is the Reynolds number, Pr is the Prandtl number, ρ is the mass density of the bulk fluid, and u_m is a characteristic velocity defined as $|\partial \sigma / \partial T| |\partial T / \partial z| (z_B / \mu)$. Length z_B (distance from the lower pole of the bubble to the solid surface) can be chosen for this velocity scale because the ranges of velocities observed in the primary vortex surrounding the bubble, for $Re < 1$, are of the same order of magnitude as the normal distance of the interface from the center of this vortex. $l = r_B$ is a characteristic length scale, μ and ν are dynamic and kinematic viscosities, respectively, and α is the thermal diffusion coefficient of the test liquid. In our experiment the Pr range has been estimated to be between 5–28 for the temperature range used. The dynamic Bond number Bo can be defined as the ratio of Rayleigh number to Marangoni number, $Bo = Ra/Ma = g \beta l^4 |\partial T / \partial r| / (\nu \alpha Ma)$, where g is the gravitational acceleration, β is the coefficient of thermal expansion, and $\partial T / \partial r$ is the horizontal temperature gradient. We note that $\partial T / \partial r$, as a characteristic gradient near the bubble, is inherently coupled with $\partial T / \partial z$. Therefore, Bo is a function of Ma and will not be evaluated independently.

A significant temperature variation exists near the bubble surface and is primarily confined to a region within one bubble height z_B of the gas–liquid interface. Because this is a characteristic length, a bubble shape parameter can be defined as $A_r = r_B / z_B$. Observations of oscillatory flow initiation have also shown that this parameter is a major factor in inducing or suppressing these instabilities. Therefore, a modified Ma is defined as $Ma_m = Ma A_r$, and has been used in the present data analysis. Hereafter, this will be referred to as the Marangoni number.

Experimental Approach

Experimental approach and liquid properties have been described in detail by Rashidnia¹¹ in a previous report. The flow-fields are visualized using a laser light sheet at the meridian plane of the bubble. The movement of aluminum particle flow tracers is recorded by a time-lapse recorder on S-VHS tapes for flow pattern and oscillation detection. The temperature fields are visualized using a Mach–Zehnder interferometer.

Discussion of Results

The presence of the temperature gradient near the bubble surface induces thermocapillary convection, which disturbs the temperature stratification near the bubble. A horizontal temperature gradient forms, resulting in a buoyancy force. The buoyancy force near the interface counteracts the thermocapillary-induced flow force. Figure 1a shows that the fringes are packed beneath the bubble. This means that the temperature gradient is higher in this region than in the regions farther from the bubble, indicating enhanced heat transport in the vertical direction beneath the bubble. The bubble surface curvature

Presented as Paper 95-0880 at the AIAA 33rd Aerospace Sciences Meeting, Reno, NV, Jan. 9–12, 1995; received May 15, 1995; revision received Jan. 10, 1997; accepted for publication Jan. 13, 1997. Copyright © 1997 by the American Institute of Aeronautics and Astronautics, Inc. No copyright is asserted in the United States under Title 17, U.S. Code. The U.S. Government has a royalty-free license to exercise all rights under the copyright claimed herein for Governmental purposes. All other rights are reserved by the copyright owner.

*Senior Scientist, NYMA, Inc. Senior Member AIAA.

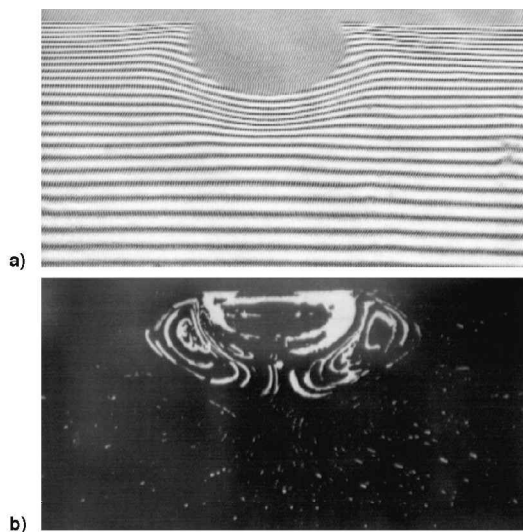


Fig. 1 Steady-state interferometric a) fringe pattern and 2) laser sheet images near the bubble.

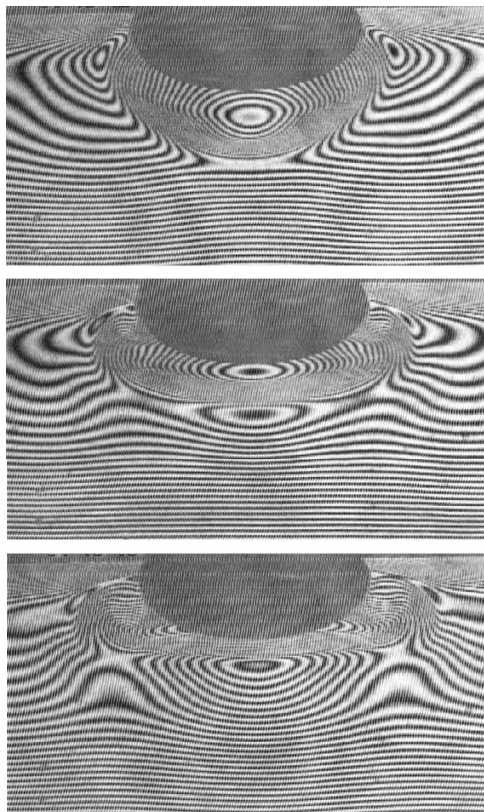


Fig. 2 Sequence of interferograms (follow in vertical direction) for symmetric oscillatory case of refractive index field near the bubble.

does not cause fringe deformation in an isothermal test condition, negating the possible lensing effect.

Transition from the steady state to an unsteady flow condition has been observed, as has the onset of oscillations for particular bubble sizes and temperature gradients. At a critical temperature gradient for a given bubble size, flow becomes oscillatory. A typical symmetric oscillation field can be observed in Fig. 2. Similarly unstable behavior has been observed in test liquids of higher Prandtl numbers. Particle flow visualization shows similar oscillations in the velocity distributions around the individual bubbles. At higher Marangoni numbers, the interferometric images reveal asymmetric oscillations as seen in Fig. 3.

At moderate temperature gradients, similar instabilities are observed as the bubble size is slowly increased. The flow undergoes a transition from steady state to various oscillatory modes when the bubble size exceeds a certain value.

Strong steady and oscillatory flows originate near the bubble surface where high thermal gradients exist. Experiments using finer increments of temperature gradient and bubble size are currently being conducted, which in conjunction with numerical models, will quantify the nature of the temperature and velocity fields surrounding the bubble, thereby pinpointing the prevailing conditions at the onset of the oscillatory modes. Consequently, only limited results of initial analyses are presented here.

For liquids of moderate Pr , steady-state flow and transitions to unsteady flow conditions are observed where Ma_m is less than 20,000. In this range of Marangoni numbers, the oscillations are not periodic because of the transient nature of the flow variations; therefore a frequency cannot be defined. At Ma_m larger than 20,000, periodic oscillations of the temperature fields near the contact line between the bubble and the heated surface are observed. The recorded oscillation frequencies lie in a rather narrow range for the temperature gradients and bubble sizes given in Table 1. Around $Ma_m = 78,000$, the flow exhibited asymmetric patterns as indicated in a typical case depicted in Fig. 3.

Nonperiodic oscillations and chaotic flow patterns are observed at Marangoni numbers estimated at 105,000. Thus, the bubble behaves quite differently in a high thermal gradient as compared to the lower thermal gradients. The bubble exhibits a horizontal jerking motion about its position. Fluid motion around the bubble becomes quite vigorous and chaotic. Neither surface deformation nor jerking of the bubble is detected in any of the cases observed at lower temperature gradients. In the chaotic regime, interferogram images become very complicated and difficult to recognize. These results have been reproduced during several months of tests using the same batch

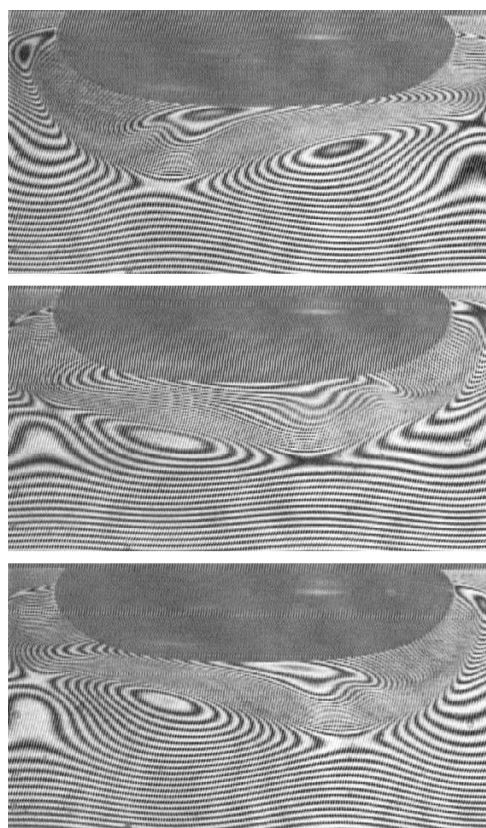


Fig. 3 Sequence of interferograms (follow in vertical direction) for asymmetric oscillatory case of refractive index field near the bubble.

Table 1 Test conditions and results

$\partial T/\partial z$, K/cm	Frequency, Hz	r_B , mm	$A_r = r_B/z_B$	$Ma_m = MaA_r$	Flow mode/regime
$Pr = 8.4$ liquid					
3.16	0.000	2.350	1.093	4,428	Steady state
3.16	0.000	4.100	1.570	19,364	Steady state
6.32	0.000	1.933	1.000	5,301	Steady state
6.32	—	2.850	1.273	15,183	Transitional
6.32	0.259	3.250	1.413	21,915	Symmetric oscillation
6.32	0.238	4.000	1.569	36,862	Symmetric oscillation
6.32	0.215	5.125	1.970	75,978	Symmetric oscillation
9.47	0.000	1.000	0.870	1,915	Steady state
9.47	—	1.625	0.985	5,725	Transitional
9.47	0.272	2.725	1.267	20,709	Symmetric oscillation
9.47	0.252	3.525	1.469	40,178	Symmetric oscillation
9.47	0.244	4.575	1.694	78,044	Asymmetric oscillation
22.0	—	3.150	2.100	106,508	Nonperiodic oscillation
$Pr = 27$ liquid					
23.16	0.000	1.550	1.033	5,572	Steady state
23.16	0.454	2.750	1.279	21,718	Symmetric oscillation
23.16	0.429	3.400	1.545	40,101	Symmetric oscillation
23.16	0.345	4.750	1.900	78,269	Asymmetric oscillation

of liquid, confirming that surface contaminants are not responsible for the observed phenomena.

Oscillation Mechanism

Consider one cycle of flow oscillation during which the gas–bubble interface experiences continuous temperature gradient variation. These temperature profiles qualitatively agree with interface temperature distributions given in earlier reports.^{8,10} Define $\nabla_s T$ and $\nabla_r T$ as tangential and radial temperature gradients at the liquid–gas interface, respectively. At the start of each cycle, $\nabla_s T$ attains its maximum value, which enables the thermocapillary (TC) convective heat transfer mode to dominate the system (bubble surface region). The TC convective flow transfers hotter liquid to the cooler regions of the bubble surface, establishing a uniform temperature, thereby reducing $\nabla_s T$. However, because the interface temperature is uniformly maximum while the rest of the cell retains its initial global gradient, $\nabla_r T$ becomes very large, enabling the conductive mode of heat transfer to dominate. Because heat is conducted away from the bubble surface faster than the TC convection can replace it, the gas–liquid interface temperature decreases nonuniformly, causing $\nabla_s T$ to increase again. This slows the conductive mode while restoring the previous mechanism for TC convection. The cycle repeats when $\nabla_s T$ attains its maximum value.

On Earth the natural convection opposes the thermocapillary flow, but in a low-gravity environment this resistance is absent. The previous mechanism suggests that oscillation will occur in reduced gravity environments. However, low-gravity experiments are essential to verify this hypothesis.

Conclusions

An experimental study has been carried out using interferometry and particle tracing to observe and demonstrate the steady, transitional, periodic and nonperiodic oscillatory thermal, and flowfields surrounding several individual air bubbles in a bulk liquid on a solid surface subjected to different temperature gradients.

The flow induced a larger temperature gradient below the colder pole of the bubbles than in an undisturbed fluid. This, in turn, was associated with a lateral temperature gradient that caused a buoyancy force capable of counteracting the thermocapillary flow force. This buoyancy force cannot be neglected and may have an effect on the instability. Periodic oscillatory temperature and flowfields were observed beyond a critical Marangoni number. A possible mechanism respon-

sible for oscillations has been given. However, it is generally known that thermocapillary flow becomes oscillatory under certain conditions, but its cause is not yet completely understood. The least understood part is the role free surface deformability plays in the oscillation mechanism. No obvious deformations of the bubble surface were observed except at the highest temperature gradient used in this experiment, which caused nonperiodic chaotic flow and caused the bubble to move violently. Neither evaporation/condensation for low ranges of thermal gradients nor contamination of the liquid seem to have caused the observed phenomena.

Acknowledgment

This project was supported by NASA Lewis Research Center under Contract NAS3-27186 with NYMA, Inc.

References

- ¹Ostrach, S., "Low-Gravity Fluid Flows," *Annual Review of Fluid Mechanics*, Vol. 14, 1982, pp. 313–345.
- ²Young, N. O., Goldstein, J. S., and Block, M. J., "The Motion of Bubbles in a Vertical Temperature Gradient," *Journal of Fluid Mechanics*, Vol. 6, 1959, pp. 350–356.
- ³Subramanian, R. S., *The Motion of Bubbles and Drops in Reduced Gravity, in Transport Processes in Bubbles, Drops and Particles*, edited by R. P. Chhabra and D. Dekee, Hemisphere, New York, 1991.
- ⁴Barton, K. D., and Subramanian, R. S., "Migration of Liquid Drops in a Vertical Temperature Gradient—Interaction Effects near a Horizontal Surface," *Journal of Colloid and Interface Science*, Vol. 141, No. 1, 1991, pp. 146–156.
- ⁵Thompson, R. L., DeWitt, K. J., and Labus, T. L., "Marangoni Bubble Motion Phenomenon in Zero Gravity," *Chemical Engineering Communications*, Vol. 5, 1980, pp. 299–314.
- ⁶Rashidnia, N., and Balasubramanian, R., "Thermocapillary Migration of Liquid Droplets in a Temperature Gradient in a Density Matched System," *Experiments in Fluids*, Vol. 11, Nos. 2/3, 1991, pp. 167–174.
- ⁷Papazian, J. M., and Wilcox, W. R., "Interaction of Bubbles with Solidification Interfaces," *AIAA Journal*, Vol. 16, No. 5, 1978, pp. 447–451.
- ⁸Raake, D., Siekmann, J., and Chun, C.-H., "Temperature and Velocity Fields Due to Surface Tension Driven Flow," *Experiments in Fluids*, Vol. 7, No. 2, 1989, pp. 164–172.
- ⁹Chun, C.-H., Raake, D., and Hansmann, G., "Oscillating Convection Modes in the Surroundings of an Air Bubble Under a Horizontal Heated Wall," *Experiments in Fluids*, Vol. 11, No. 5, 1991, pp. 359–367.
- ¹⁰Kassemi, M., and Rashidnia, N., "Thermocapillary and Natural Convective Flows Generated by a Bubble in 1-G and Low-G Environments," AIAA Paper 96-0734, Jan. 1996.